CONFERENCE PAPERS

EXPECTED AND OBSERVED CHANGES TO DESCRIPTORS OF TRABECULAR ARCHITECTURE WITH AGING – A COMPARISON OF MEASUREMENT TECHNIQUES

A. Badiei[1,2], M.J. Bottema[3], and N.L. Fazzalari[1,2]

[1]*Bone & Joint Research Laboratory, Institute of Medical & Veterinary Science (IMVS), Adelaide, Australia*

[2]*Department of Pathology, University of Adelaide, Adelaide, Australia*

[3]*School of Informatics & Engineering, Flinders University, Adelaide, Australia*

arash.badiei@imvs.sa.gov.au

Abstract

The fragility of trabecular bone depends not only on the amount of bone but also on its architecture. In order to assess fragility of bone, describe changes due to age, and monitor effect of disease or treatment, it is necessary to model the physical properties of trabecular bone architecture. An important feature of bone architecture is the degree of anisotropy (DA). Estimates of DA may be obtained from computed tomography data by characterizing orientation in images. Widely used image descriptors for estimating orientation in this setting include mean intercept length (MIL), line fraction deviation (LFD), star length distribution (SLD) and star volume distribution (SVD). In this study, estimates of DA computed via each of these image descriptors are compared on synthetic images for various combinations of trabecular thickness, separation and number. Estimates of DA are also computed for real images representing different stages of aging. It is found that estimates of DA vary substantially depending on the choice of image descriptor. In particular, the MIL tends to underestimate DA.

Introduction

The bone at articular joints, vertebral body and pelvis are composed, in part, of a porous material called trabecular bone (Figure 1). The fragility or mechanical competence of trabecular bone depends not only on the amount of bone but also on its architecture.

In the 19th century Meyer and Wolff observed that trabecular bone architecture was highly influenced by trabecular bone mechanics, implying that trabecular architecture exhibited preferential alignment corresponding to stress trajectories[1]. The consequence of this observation (Wolff's law) is that information regarding trabecular bone mechanics is reflected in the trabecular architecture. This relationship is depicted most clearly in the anisotropy or preferential alignment of the trabecular bone (Figure 1).

In order to estimate fragility of bone, describe changes due to age, and monitor effect of disease or treatment, it is necessary to model the physical properties of cancellous bone in terms of the architectural structure. Commonly used descriptors of this architecture include trabecular thickness (Tb.Th), separation (Tb.Sp), number (Tb.N), and degree of anisotropy (DA).

Direct measurement of these descriptors is prohibitively invasive in a clinical setting. Accordingly, these parameters must be estimated from data such as computed tomography images. This process introduces a second layer of modeling; the association of architectural parameters with image features. The most widely used method for this task is based on the Parfitt plate-model[2], where trabecular bone architecture is modeled as parallel plates (Figure 2). This model provides access to analysis of the complex trabecular architecture, and is an adopted tool in the bone research community[2, 3].

Architectural anisotropy is most commonly measured using the mean intercept length (MIL)[1,4-6]. Other methods such as the line fraction deviation (LFD), star length distribution (SLD) and star volume distribution (SVD) have also been implemented by various investigators[1, 7, 8]. These methods will be described in section 2.

It has been widely reported that a number of trabecular architectural changes occur with age[3, 9-14]. In this study estimates of DA computed via each of the descriptors (MIL, LFD, SLD and SVD) are compared on synthetic images for various combinations of trabecular Tb.Th, Tb.Sp and Tb.N. Estimates of DA are also computed for real images representing different stages of aging.

Anisotropy Measures

Mean Intercept Length

Whitehouse[5] was one of the first investigators to introduce the concept of the mean intercept length (MIL) to the study of the anisotropic properties of trabecular bone. The MIL is the mean distance between two bone/ marrow interfaces[1,8]. The fundamental principles of this technique arise from the field of stereology and the underlying mathematics (integral geometry) may be viewed as a variation of "Buffon's needle problem"[15, 16]. The computation of the MIL consists of the sampling (counting) of intersections between a sampling grid and the bone/ marrow interface as a function of the grid's orientation, ϕ[1]. The MIL can be expressed as

$$\mathrm{MIL}(\phi) = \frac{L}{I(\varphi)}, 0^{o} \le \phi < 180^{o} \qquad (1)$$

where MIL (ϕ) is the mean intercept length component at orientation ϕ, L is the total length of the sampling grid

and $I(\phi)$ is the number of intercepts sampled at orientation ϕ.

Line Fraction Deviation

The line fraction deviation (LFD) was introduced by Geraets et al[7] as an index of orientation applied to segmented radiographic images of trabecular networks. The LFD is the standard deviation of the fraction of trabecular bone pixels within a grid[7, 17]. In the segmented image, if the trabecular bone pattern aligns with respect to the grid, a larger standard deviation will be recorded compared to when the trabecular bone pattern does not align with respect to the grid[17, 18]. This, in effect, captures architectural anisotropy information.

Star Volume Distribution

The star volume distribution (SVD) technique was introduced by Cruz-Orive et al[19] and is closely related to the star volume defined by Gundersen & Jensen[8, 20]. The SVD describes the typical distribution of trabecular bone around a typical point in a trabecula. The SVD is the mean volume of a trabecula seen unobstructed from a random point within the trabecula, evaluated as a function of orientation. If sampling at random points is replaced by sampling on a grid, the SVD is given by

$$SVD(\phi) = \frac{\pi}{3} \frac{\sum_{i=1}^{n} (Li(\phi))^4}{\sum_{i=1}^{n} (Li(\phi))}, 0^o \le \phi < 180^o \quad (2)$$

where SVD (ϕ) is the star volume component at orientation ϕ and L_i is the length of the intersection i of a grid line with a trabecular structure[8].

Star Length Distribution

The star length distribution (SLD) was introduced by Odgaard et al[21] as a slight modification on the SVD[1, 8, 22]. SLD employs a similar computational procedure as the SVD with the addition of weighting by the observed intersection length. If sampling at random points is replaced by sampling on a grid, the SLD is given by

$$SLD(\phi) = \frac{\sum_{i=1}^{n} (L_i(\phi))^2}{\sum_{i=1}^{n} Li(\phi)}, 0^o \le \phi < 180^o \quad (3)$$

where SLD (ϕ) is the star length component at orientation ϕ and L_i is the length of the intersection i of a grid line with the trabecular structure[8].

Materials and methods

Four micro-computed tomography (μCT) sections of human cadaveric vertebral (L2) trabecular bone and eight synthetic images were analysed. Binary synthetic images were constructed with simple geometries to mimic changes occurring in vertebral trabecular architecture (Figures 3 and 5). Trabecular bone cubes (10mm) were harvested from the central region of L2 vertebrae of four female subjects (ages 33, 56, 76 and 87 years) and imaged using μCT modality (Skyscan 1072, Skyscan, Belgium). Four random sections from each μCT dataset were selected for analysis (Figure 7). The grey tomographic images were binarised using a global thresholding algorithm. Optimal thresholds were selected using Otsu's method[23] based on the grey-level histogram of each individual image (Figure 3). Following binarisation morphological open and close operations were performed to remove isolated pixels. All image processing tasks were carried out using functions available in the Matlab Image Processing Toolbox (Mathworks, Massachusetts).

CTAnalyzer software (Skyscan, Belgium) was used to derive structural parameters (Tb.Th, Tb.Sp and Tb.N) of images from two-dimensional measurements of bone mineral perimeter (BS), bone mineral area (BV) and bone tissue area (TV) by the plate-model (Figure 2) using the following formulas[2].

$$Tb.N = 0.5 x BS / TV \quad (4)$$

$$Tb.Th = \left(\frac{BV / TV}{\frac{100}{Tb.N}} \right) \quad (5)$$

$$Tb.Sp = \left(\frac{1 - \left(\frac{BV / TV}{100} \right)}{Tb.N} \right) \quad (6)$$

BS/TV represents the total bone mineral surface and BV/TV represents the bone volume fraction. BS/TV and the MIL have a reciprocal relationship ($\frac{BS}{TV} = \frac{1}{MIL}$), since BS/TV can also be determined using the same process used for computation of the MIL[24].

The DA was computed as the ratio of maximum eigenvalue to minimum eigenvalue of the best fitting ellipse to the anisotropy data obtained from each of the four measures (MIL, LFD, SLD and SVD). For comparison, the DA from each set of tests was normalised with respect to the maximum DA of a group. All anisotropy analyses were performed using custom written software in Matlab.

Results

Trabecular Thickness

The images shown in Figure 3 were used to investigate the effects of changes in trabecular thickness to DA. In this sequence the horizontal element thins while the vertical element thickens. Table 1 shows the corresponding plate-model architectural parameters for the structures shown in Figure 3. Figure 4 shows the resulting DA measurements. The MIL detects no

difference in DA, whereas the LFD, SLD and SVD show increasing DA with changes in Tb.Th. The LFD, SLD and SVD all show the same trend in DA for the structures analysed.

Trabecular Number

The images shown in Figure 5 were used to investigate the effects of changes to trabecular number on the DA. In this sequence horizontal and vertical trabecular elements are sequentially removed from the overall structure. Table 2 shows the corresponding plate-model architectural parameters for the structures shown in Figure 5. Figure 6 shows the resulting DA measurements. All descriptors show increasing DA to varying degrees. The MIL and LFD show the least sensitivity, while the SVD shows the greatest sensitivity to changes in Tb.N.

Aging Bone

The images shown in Figure 7 were used to investigate the changes to DA that may occur as a result of changes to trabecular architecture with aging. Table 3 shows the corresponding plate-model architectural parameters for the structures shown. Figure 8 shows the resulting DA measurements. All measures show different interpretations of DA. The MIL, LFD and SLD give the structure in image D (Figure 7) the highest weighting, while the SVD does not. Similarly the LFD, SLD and SVD give the structure in image B (Figure 7) a higher weighting than the MIL.

Discussion

Changes to Tb.Th and subsequent changes to DA can be underestimated or missed using information from MIL based measures of anisotropy. Other architectural changes, such as changes to Tb.N and Tb.Sp, may also be represented differently by different measurement techniques. It is therefore important to understand the nature of the measurements being made by various techniques.

Many researchers have observed changes in vertebral Tb.Th with aging. Mosekilde[11, 25] found that the mean horizontal Tb.Th decreased significantly with age, whereas mean vertical Tb.Th was independent of age without any gender bias. More recently Thomsen et al[3] also found horizontal Tb.Th decreased significantly with age while mean vertical Tb.Th was independent of age. Others[26,27] have also suggested that with age related changes to vertebral architecture extra load maybe presented to remaining architectural elements. This load could potentially trigger adaptive changes in the bone resulting in the thickening of vertical architectural elements[3, 26, 27]. This notion is supported by the results of Atkinson[13] who found vertical trabecular elements increase in width with age.

The thinning of horizontal trabeculae and thickening of vertical trabeculae will increase the DA. This is due to the fact that through these changes more bone material will be aligned vertically than horizontally. The MIL based measures exhibited the least sensitivity to changes in Tb.Th (Figure 4). While the other measures (LFD, SLD & SVD) all characterised the changes to varying degrees (Figure 4). The insensitivity of the MIL based measure is due to the fact that the MIL characterises surface distribution[1]. Changes to thickness results in little to no change to the overall surface distribution of a structure. Thus, changes to Tb.Th can be underestimated or missed using a MIL based measure. Since the LFD, SLD and SVD shift focus of measurement away from surface to the material itself[1,8,21] any changes to the distribution of material will be characterised. As such, the LFD, SLD and SVD all show increasing DA with changes to Tb.Th (Figure 4). With a decrease in BV/TV and little to no change in BS/TV, plate-model parameters should show corresponding changes, namely, decrease in Tb.Th, increase in Tb.Sp and little to no change in Tb.N. This trend was observed (Table 1) for the structures shown in Figure 3.

In 1967, Atkinson[13] demonstrated that horizontal trabeculae of the vertebral body decreased in number though out life. In the 1980s Pêrteux et al[28] found the ratio of vertical to horizontal trabeculae increased with age. More recently Thomsen et al[3] demonstrated a decrease of both horizontal and vertical trabeculae with age, while Gong et al[12] were able to demonstrate similar changes in a Chinese population.

Loss of trabecular elements leading to a decrease in the Tb.N will affect DA. This is due to the fact that if material in a given direction is decreased then the overall preferential alignment of the sample has been altered. This is visually evident in Figure 5. Changes to Tb.N also result in changes in BV/TV, BS/TV and bone segment lengths. As such, all four measures of anisotropy were able to characterise the changes (Figure 6). The notable features of this result are that the MIL and LFD show very similar results between all structures, whereas the SLD and SVD weigh the last structure (Figure 5, bottom-right) much more than the remaining three structures. This could be due to absence of smaller bone segments in the last structure. Changes to BV/TV and BS/TV will also result in changes to plate-model parameters. Table 2 shows the changes in Tb.Sp and Tb.N that were captured. However, changes in Tb.Th were also observed, even though no physical change to Tb.Th occurred.

The architectural changes shown in Figures 3 and 5 do not occur in isolation. Changes to Tb.Th, Tb.Sp and Tb.N are likely to have a complex relationship that are also linked to alterations in the DA[3,10-12]. Figure 7 illustrates the type of changes to trabecular architecture that are visually evident with aging. The corresponding plate-model parameters (Table 3) illustrate a trend in agreement with findings of other investigators. Namely, a decrease in BV/TV[11, 12], a decrease in Tb.Th[3, 10, 14, 26, 29], an increase in Tb.Sp[3, 10, 11] and a decrease in Tb.N[3, 28, 30] with age.

However, all four measures of anisotropy gave different accounts of the changes in anisotropy with aging

(Figure 8). DA measures based on the MIL are in agreement with findings by other investigators, namely the DA increases with age[9, 12]. However, the LFD, SLD and SVD all show different trends in DA. The LFD and

SLD characterise the 87-year-old sample as the most anisotropic, in accordance with the MIL. The SVD however characterised the 56-year-old sample as the most anisotropic of the group. The LFD and SLD both highlight this 56-year-old structure as the second most anisotropic of the group. Inspection of the images in Figure 7 reveals a prominent trabecular structure on the center-left part of the image of the 56-year-old sample. While the LFD, SLD and SVD give this prominent structure high weighting the MIL does not.

This brings up an important point that was also highlighted by Odgaard[1]. With the existence of such a variety of measures of anisotropy, one must define clearly the architectural property of interest being analysed. Hence, the trends in DA illustrated in Figure 8 are based on the architectural properties that each technique (MIL, LFD, SLD and SVD) measures. As such one cannot say that one technique is correct. A more fundamental question would be which of these anisotropy measures best describes the mechanical competence and hence fragility of the trabecular bone. The discussion of this is beyond the scope of this study.

This study has highlighted the importance of understanding the tools one uses in the analyses of trabecular architecture. In order to estimate fragility of bone, describe changes due to age, and monitor effects of disease or treatment, it is vital to understand and interpret results of different analyses correctly. At present, there are many tools available for the assessment of trabecular architecture. Each tool measures certain properties of the trabecular architecture; hence it is important to recognize the strengths and weaknesses of the tools one uses, especially during interpretation of results.

References

1. Odgaard, A., Three-dimensional methods for quantification of cancellous bone architecture. Bone, 1997. 20(4): p. 315-28.
2. Parfitt, A., et al., *Relationship between surface, volume and thickness of iliac trabecular bone in aging and in osteoporosis.* Journal of Clinical Investigation, 1983. 72: p. 1396-1409.
3. Thomsen, J.S., E.N. Ebbesen, and L.I. Mosekilde, *Age-related differences between thinning of horizontal and vertical trabeculae in human lumbar bone as assessed by a new computerized method.* Bone, 2002. 31(1): p. 136-42.
4. Chappard, C., et al., *Anisotropy changes in post-menopausal osteoporosis: characterization by a new index applied to trabecular bone radiographic images.* Osteoporosis Int, 2005.
5. Whitehouse, W.J., *The quantitative morphology of anisotropic trabecular bone.* J Microsc, 1974. 101 Pt 2: p. 153-68.
6. Harrigan, T.P. and R.W. Mann, *Characterization of Microsturctural Anisotropy in Orthotropic Materials Using a Second Rank Tensor.* Journal of Material Science, 1984. 19: p. 761 - 767.
7. Geraets, W.G., et al., *Orientation of the trabecular pattern of the distal radius around the menopause.* J Biomech, 1997. 30(4): p. 363-70.
8. Smit, T.H., E. Schneider, and A. Odgaard, *Star length distribution: a volume-based concept for the characterization of structural anisotropy.* J Microsc, 1998. 191 (Pt 3): p. 249-57.
9. Mosekilde, L., *Normal vertebral body size and compressive strength: relations to age and to vertebral and iliac trabecular bone compressive strength.* Bone, 1986. 7(3): p. 207-12.
10. Mosekilde, L., *Age-related changes in vertebral trabecular bone architecture--assessed by a new method.* Bone, 1988. 9(4): p. 247-50.
11. Mosekilde, L., *Sex differences in age-related loss of vertebral trabecular bone mass and structure--biomechanical consequences.* Bone, 1989. 10(6): p. 425-32.
12. Gong, H., et al., *Regional variations in microstructural properties of vertebral trabeculae with aging.* J Bone Miner Metab, 2005. 23(2): p. 174-80.
13. Atkinson, P.J., *Variation in trabecular structure of vertebrae with age.* Calcif Tissue Res, 1967. 1(1): p. 24-32.
14. Oda, K., et al., *Morphogenesis of vertebral deformities in involutional osteoporosis. Age-related, three-dimensional trabecular structure.* Spine, 1998. 23(9): p. 1050-5, discussion 1056.
15. Kanatani, K., *Measurement of Particle Orientation Distribution by a Stereological Method.* Part. Charact., 1985. 2: p. 31 - 37.
16. Russ, J.C. and R.T. Dehoff, *Practical Stereology*. 2 ed. 2000, New York: Plenum Publishers.
17. Geraets, W.G., *Comparison of two methods for measuring orientation.* Bone, 1998. 23(4): p. 383-8.
18. Geraets, W.G., et al., *A new method for automatic recognition of the radiographic trabecular pattern.* J Bone Miner Res, 1990. 5(3): p. 227-33.
19. Cruz-Orive, L.M., et al., *Characterizing Anisotropy: A New Concept.* Micron and Microscopica Acta, 1992. 23(1 - 2): p. 75 - 76.
20. Gundersen, H.J. and E.B. Jensen, *Stereological Estimation of the Volume-Weighted Mean Volume of Arbitrary Particles Observed on Random Sections.* Journal Of Microscopy, 1985. 138(2): p. 127 - 142.
21. Odgaard, A., et al., *Fabric and elastic principal directions of cancellous bone are closely related.* J Biomech, 1997. 30(5): p. 487-95.
22. Ketcham, R.A. and T.M. Ryan, *Quantification and Visualization of Anisotropy in Trabecular Bone.* Journal Of Microscopy, 2004. 213(2): p. 158 - 171.

23. Otsu, N., *A Threshold Selection Method from Gray-Level Histograms.* IEEE Transactions on Systems, Man, and Cybernetics, 1979. 9(1): p. 62 - 66.
24. Parfitt, A.M., *Bone Histomorphometry: Techniques and Interpretation*, ed. R.R. Recker. 1983: CRC Press.
25. Mosekilde, L., et al., *Trabecular bone structure and strength - remodelling and repair.* J Musculoskelet Neuronal Interact, 2000. 1(1): p. 25-30.
26. Frost, H.M., *On the trabecular "thickness"-number problem.* J Bone Miner Res, 1999. 14(11): p. 1816-21.
27. Parfit, A., et al., *Relationship between surface, volume and thickness of iliac trabecular bone in aging and in osteoporosis.* Journal of Clinical Investigation, 1983. 72: p. 1396-1409.
28. Preteux, F., C. Bergot, and A.M. Laval-Jeantet, *Automatic quantification of vertebral cancellous bone remodeling during aging.* Anat Clin, 1985. 7(3): p. 203-8.
29. Kothari, M., et al., *Measurement of intraspecimen variations in vertebral cancellous bone architecture.* Bone, 1999. 25(2): p. 245-50.
30. Twomey, L., J. Taylor, and B. Furniss, *Age changes in the bone density and structure of the lumbar vertebral column.* J Anat, 1983. 136 (Pt 1): p. 15-25.

Tables

Table 1. *Plate-model architectural parameters for the structures shown in Figure 3.*

Image	BV/TV (%)	Tb.Th (Pixels)	Tb.Sp (Pixels)	Tb.N (1/Pixels)
TbNA	8.45	3.18	34.43	0.027
TbNB	7.87	3.16	36.93	0.025
TbNC	7.31	3.13	39.73	0.023
TbND	6.50	3.10	44.60	0.021

Table 2. *Plate-model architectural parameters for the structures shown in Figure 5.*

Image	BV/TV (%)	Tb.Th (Pixels)	Tb.Sp (Pixels)	Tb.N (1/Pixels)
A	22.59	9.74	33.37	0.023
B	13.00	9.28	62.11	0.014
C	10.88	7.61	62.31	0.014
D	9.01	9.24	93.28	0.01

Table 3. *Plate-model architectural parameters for the structures shown in Figure 7.*

Image	BV/TV (%)	Tb.Th (Pixels)	Tb.Sp (Pixels)	Tb.N (1/Pixels)
TbThA	6.56	13.12	184.14	0.005
TbThB	6.47	12.77	184.49	0.005
TbThC	6.32	12.47	184.79	0.005
TbThD	6.25	12.33	184.92	0.005

Illustrations

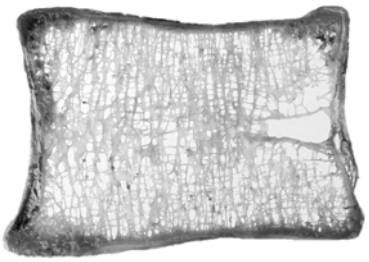

Figure 1. *Coronal section of a human vertebral body illustrating preferential alignment (anisotropy) of trabecular bone architecture.*

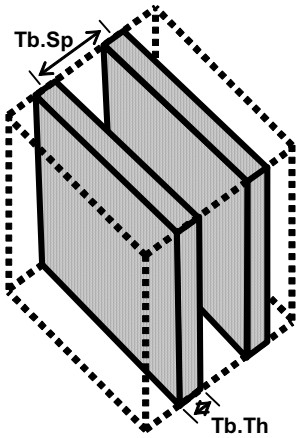

Figure 2. *Diagram illustrating the Parfitt plate-model. Two parallel plates, each with a surface area of 1 mm2 on each side, contained within a cube with sides of length 1 mm.*

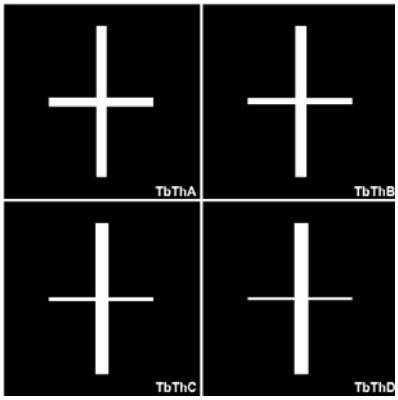

Figure 3. *Sequence of images used to investigate the effects of Tb.Th on DA with minimal BV/TV change.*

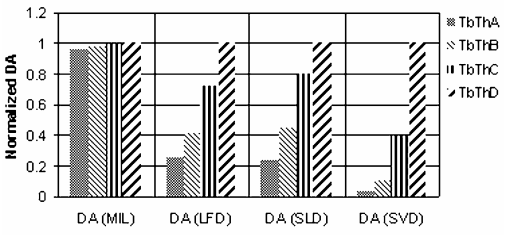

Figure 4. *Normalised DA of structures shown in Figure 3.*

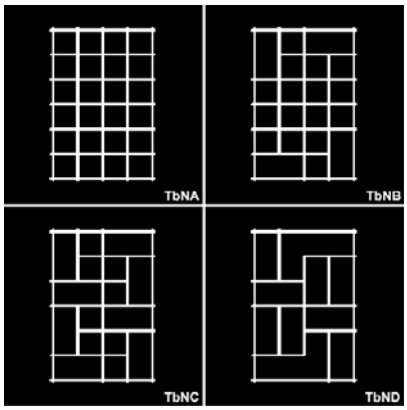

Figure 5. *Sequence of images used to investigate the effects of decreasing Tb.N on DA with associated BV/TV decrease.*

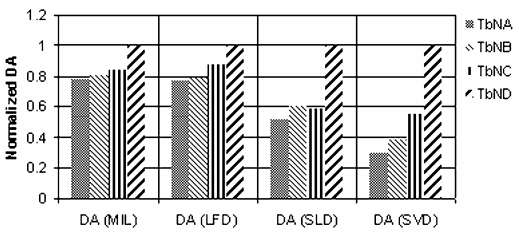

Figure 6. *Normalised DA of structures shown in Figure 5.*

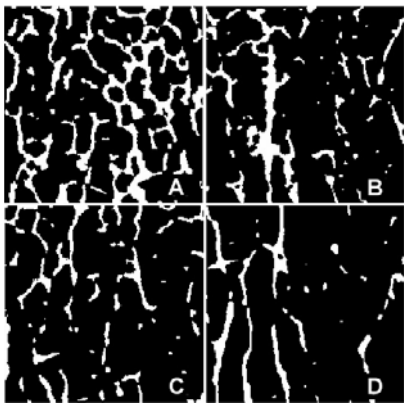

Figure 7. *Sequence of images used to investigate the effects of aging on DA, (A) 33 years old, (B) 56 years old, (C) 76 years old and (D) 87 years old.*

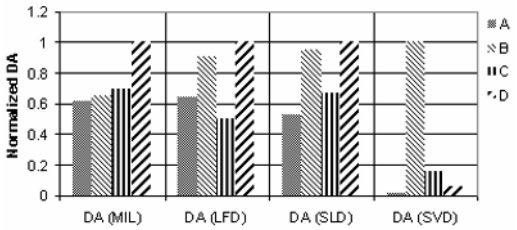

Figure 8. *Normalised DA for the structures shown in Figure 7.*

A NEW VERSATILE HAND DYNAMOMETER

[1]Darius Chapman, [2]Nicola Massy-Westropp, [1]Trevor C Hearn, [1]Karen J Reynolds

[1]*School of Informatics & Engineering, Flinders University, South Australia*

[2]*Division of Health Sciences, University of South Australia*

Abstract

This paper describes the design and testing of a new hand strain-gauge based dynamometer. The design is portable and capable of measuring grip strengths from 12.5 to 800N. The dynamometer is independent of point of application of the grip force. Finite element modelling and experimental testing were used to verify the mechanical system's suitability. The dynamometer was designed for input to a PDA to allow full portability of the device.

Keywords: Hand dynamometer, hand grip strength, rheumatoid arthritis

Introduction

Studies have shown that hand grip strength plays an important role in classification and diagnosis of various pathologies. Grip strength can be associated with bone density, a predictor of incident disability and a classifier of the severity of hand injuries and associated pathologies such as Rheumatoid Arthritis (RA)[i,ii] [iii] Instrumentation for measuring grip-strength transfers physical function into quantitative data to help map and diagnose various conditions.

There are four main types of instrumentation used to measure grip strength, as reported in a *Literature Review of Grip Strength Testing*[iv]; Hydraulic, Pneumatic, Mechanical and Strain Gauge. The most widely used and reported is the Jamar Hydraulic Dynamometer (Asimow Engineering, CA, USA) that uses two pressure gauges to drive an analogue meter. Other instruments are also available that use similar techniques to the Jamar. These all measure peak grip strength, recorded by a floating needle on the meter. However, other grip tests, such as endurance, are not able to be measured with these instruments.

While the Jamar is reported to be a reliable instrument for normal grip measurement, its design is not suited to low strength testing, or people suffering RA. In a published study, this device failed to register any force for some patients[6]. The minimum recordable grip force on the Jamar is 25N while some RA patients are only able to